ACS Catalysis

Article

Electrochemically generated copper carbonyl for selective dimethyl carbonate synthesis

Bethan Jane Venceslau Davies, Manuel Šari#, Marta C Figueiredo, Niels C Schjødt, Søren Dahl, Poul Georg Moses, Maria Escudero-Escribano, Matthias Arenz, and Jan Rossmeisl

ACS Catal., **Just Accepted Manuscript** • DOI: 10.1021/acscatal.8b03682 • Publication Date (Web): 14 Dec 2018

Just Accepted

ACS Publications

is published by the American Chemical Society. 1155 Sixteenth Street N.W., Washington, DC 20036

Electrochemically generated copper carbonyl for selective dimethyl carbonate synthesis

Bethan J. V. Davies[1], Manuel Šarić[1, 2], Marta C. Figueiredo[1]†, Niels C. Schjødt[3], Søren Dahl[3], Poul Georg Moses[3], María Escudero-Escribano[1], Matthias Arenz[1, 4]*, Jan Rossmeisl[1]**

[1]Nano-Science Center, Department of Chemistry, University of Copenhagen, Universitetsparken 5, 2100 Copenhagen, Denmark. [2]Center for Atomic Scale Materials Design (CAMd), Department of Physics, Technical University of Denmark, Fysikvej building 307, 2800 Kongens Lyngby, Denmark. [3]Haldor Topsøe A/S, Nymøllevej 55, 2800 Kongens Lyngby, Denmark. [4]Department of Chemistry and Biochemistry, University of Bern, Freiestrasse 3, 3012 Bern, Switzerland

KEYWORDS copper, dimethyl carbonate, electrosynthesis, spectroelectrochemistry, methanol

ABSTRACT

Development of electrochemical synthesis routes for high-value chemicals could pave the way for a sustainable chemical industry based on electricity. Herein, the electrochemical synthesis of the industrially relevant and environmentally benign reagent, dimethyl carbonate is investigated. By utilizing a combination of electrochemical techniques, *in situ* infrared spectroscopy and headspace-gas chromatography-mass spectrometry we show production and spectroelectrochemical evidence for the synthesis of DMC via an electrochemically generated copper carbonyl species. The formation of the copper carbonyl has close to 100% current efficiency, in the applied potential range of 0.1 – 0.4 V vs SCE. Subsequent formation of DMC

occurs with a slow reaction time on the order of 30-40 days. Relative to potential co-products, the reaction is highly selective for DMC. Optimization of the reaction may lead to a viable method of DMC production.

INTRODUCTION.

Organic electrosynthesis has the potential to replace current environmentally harmful synthesis methods of the chemical industry[1–3]. Electrosynthesis uses inherently clean electrons as the redox reagent, rather than aggressive chemicals. Electrosynthesis also generally generates less waste from spent reagents than stoichiometric or catalytic processes. Traditional chemical synthesis methods rely on fossil fuels as the energy source, whereas the energy input to drive the electrochemical reaction can be sourced from renewables, such as wind or solar.

Dimethyl carbonate (DMC) is a versatile chemical; it is environmentally benign and an industrially relevant chemical reagent and solvent[4]. Moreover, DMC is a value-added product of methanol and has potential to replace toxic phosgene and methyl halides for carbonylation and methylation, respectively. Replacement with DMC would transform such processes into Green Chemistry synthesis reactions[5–9]. DMC is also used as an electrolyte component in lithium ion batteries[10]. Since the demand for energy storage by the use of batteries is increasing[11], the production of DMC is likely to concomitantly increase[12].

The current industrial methods for producing DMC are energy intensive and hazardous, requiring high temperature and pressure to drive the reaction[13,14]. They also use dangerous combinations of reactants (CO and O_2 or NO_x)[2,3]. From a Green Chemistry perspective, these conditions and reactant combinations should be avoided and there has been increasing investigation into alternative and electrochemical methods for DMC synthesis[15]. Electrochemical synthesis of DMC uses the electrochemical potential as the driving force, rather than high temperature and high pressure[16,17]. The synthesis reactions of DMC performed

by electrochemical and chemical oxidation methods are shown in Equation 1 and Equation 2 respectively[18].

Equation 1

$$2CH_3OH + CO \rightarrow (CH_3O)_2CO + 2H^+ + 2e^-$$

Equation 2

$$2CH_3OH + CO + \frac{1}{2}O_2 \rightarrow (CH_3O)_2CO + H_2O$$

Possible co-products of the reaction are dimethyl oxalate (DMO), dimethyl ether (DME), dimethoxymethane (DMM), and methyl formate (MF)[16,19–22]. Direct oxidation of methanol to CO_2 as a competing reaction is also often observed[16,19–22]. The by-product for the chemical synthesis (Equation 2Equation 1) is water, which is waste and requires treatment. The by-products for the electrochemical synthesis on the other hand are "clean" protons and electrons[2] (Equation 1Equation 2Equation 2). These by-products could be used to make hydrogen, a valuable fuel. Reducing the amount of waste products is a step towards a more environmentally friendly chemical industry.

Electrosynthesis of DMC has been performed by a variety of techniques and with a wide range of materials. Metallic gold and palladium have both been shown to be active for electrocatalytic synthesis of DMC[16,19,20,22–24] and the surface reactions of these metals have been well studied by in-situ spectroscopy[24]. Various metal compounds have also shown to be promising as electrode materials, such as $PdCl_2$ and $CuCl_2$[21,25], as well as indirect electrochemical systems based on solution phase redox mediators such as the Br_2/Br^- system[20,26]. However, as far as the authors are aware, there has been no commercial application of electrochemical synthesis of DMC as of yet.

Herein, we continue the search for alternative and electrochemical methods of DMC synthesis by using a combination of theory and experiment. Guided by theoretical calculations on potentially suitable electrode materials, experimental investigations are performed on copper electrodes.

RESULTS AND DISCUSSION.

Thermodynamic analysis.

To investigate suitable electrode materials for electrocatalytic synthesis of DMC, thermodynamic analysis of the reaction was performed using density functional theory (DFT). Electrocatalytic synthesis of DMC requires adsorption of the reactants to the electrode surface. Adsorption energies of methoxy and carbon monoxide were selected as descriptors for the synthesis reaction of DMC on an electrode surface. The analysis focused on the energy efficiency of the reaction so that a better catalyst, in energy terms, than Au and Pd could be found. Energy efficiency is indicated by the ability to run the synthesis at a low potential. The applied potential is used for activation of methanol by the electrode to methoxy (CH_3O^*), which leads to production of DMC (Equation 3) (* indicates a surface adsorbed species or vacant surface site). From the DFT analysis it is concluded that the potential (in V vs RHE) which needs to be applied to activate methanol corresponds to the adsorption energy of methoxy (in eV). Details of the DFT calculations can be found in the Supplementary Information.

Equation 3

$$2CH_3O^* + CO^* \leftrightarrow CH_3OCOOCH_3 + 3*$$

A good catalyst candidate should bind methoxy strongly to lower the overpotential for methanol oxidation and bind CO to obtain a coverage of CO*. However, the catalyst should on the other hand bind CO* and methoxy weak enough that the intermediates to not block the surface and reaction 3 is fast. A promising metal balancing both requirements is Cu (adsorption

energy of methanol is 0.3 eV) as it activates methanol at a potential much lower than both Au (1.3 eV) and Pd (0.8 eV). This lower required potential indicates that copper should be more energy efficient than both Au and Pd. Following this analysis, copper was chosen as an electrode material to be investigated experimentally for electrochemical DMC synthesis.

Electrochemical activity.

The electrochemical activity of an electrode can be investigated by use of cyclic voltammetry. In cyclic voltammetry, a set potential range is scanned from one end to the other and back with a defined scan rate. Oxidation and reduction reactions can be observed by changes in the current response, by positive and negative signals respectively. In Figure 1 the cyclic voltammograms (CV) for a copper wire electrode recorded in an argon-saturated and CO-saturated electrolyte solution of 0.1 M $NaClO_4$ in methanol are presented. The potential range was scanned between -0.8 and 0.8 V vs. SCE at a rate of 100 mV/s. In the CV recorded with an argon-saturated electrolyte, peaks are observed for both oxidation and reduction reactions labelled as Ox1, Ox2 and Red1, Red2 respectively. The oxidation peaks are due to the formation of various copper oxides and hydroxides in the form of Cu(I), Cu(II), whereas the reduction peaks can be assigned to the reduction of these oxide species to form Cu(I) and Cu(0)[27,28]. Additionally, oxidation of the solvent, methanol, likely occurs from Ox1 onwards as well as copper dissolution. The reaction peaks indicate a degree of reversibility for some of the oxidation processes recorded, however, as the oxidation peak area is visibly larger than the reduction peak area, irreversible reactions are likely occurring, such as the oxidation of the solvent. The CV is comparable to that recorded in a similar electrolyte solution, where a broad oxidation peak is shown in the forward scan and a smaller reduction peak observed in the reverse scan[29].

On the addition of carbon monoxide (CO) gas to the electrolyte solution, a large oxidation peak Ox3 appears (Figure 1). The onset of this peak is before the onset of copper

oxidation observed without CO present in the argon saturated electrolyte solution. This peak covers the range of copper oxides/hydroxides formation. The continued presence of the two reduction peaks Red1 and Red2, indicates that the oxidation of copper still occurs and is unaffected by the new CO induced oxidation reaction. There is no corresponding reduction peak for the oxidation peak Ox3, indicating that it is an irreversible reaction. The Ox3 reaction is highly active in the methanol electrolyte solution and a comparable response is not observed for an aqueous electrolyte solution on the addition of CO (see Supplementary Information for CVs in 0.1 M $NaClO_4$(aq)).

The CO initiated oxidation process shows passivation from about 0.4 V on the forward scan and hysteresis between the two scan directions. This is suggestive of a surface deactivation at post peak potentials on the forward scan which is reactivated on the reverse scan at a lower potential. This is not an uncommon observation for the oxidation of alcohols or small organic molecules over metal surfaces. Oxidation products can cover the surface, passivating it towards further reactions. On the reverse scan, the products desorb or get reduced, so that the surface becomes available for reaction again[30].

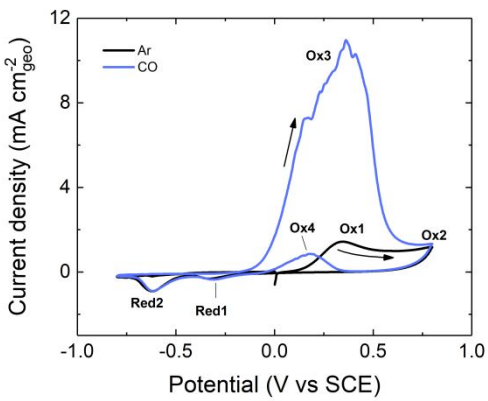

Figure 1. Cyclic voltammograms recorded with a wire copper electrode in an argon (black) and carbon monoxide (blue) saturated electrolyte solution of 0.1 M $NaClO_4$ in methanol. The potentials were scanned at a rate of 100 mV/s, in the directions indicated by the arrows. The

counter electrode was copper mesh and the reference potential was a saturated calomel electrode (SCE). Geometrical current densities are presented.

Spectroelectrochemistry.

Spectroelectrochemistry was performed using Fourier-transform infrared spectroscopy (FTIR) coupled with electrochemistry. An electrode of polycrystalline copper was used to study surface reactions, including formation of intermediates and products. Spectra were recorded at different electrode potentials in the electrochemically active range of copper in a CO environment (0.0 to 0.5 V vs. SCE), as determined to be the potential range of interest from the CV in Figure 1. Figure 2 shows the FTIR spectra in both argon-saturated (A) and CO-saturated (B) electrolyte solutions.

In an argon-saturated atmosphere (Figure 2A) five main bands are observed, at 2341, 2053, 2025-2019, 1372 and 1145 cm^{-1}. The positive band at 1145 cm^{-1} is due to ClO_4^- ions from the supporting electrolyte. As the electrode potential is made more positive, the negatively charged ClO_4^- ions concentrate in the vicinity of the electrode and consequently, the thin layer, leading to the observed increase in the band intensity. The band at 2053 cm^{-1} can be assigned to an overtone from methanol[24]. The fact that it appears as a negative feature at potentials higher than 0.2 V vs. SCE suggests that methanol decomposition starts in this potential range. In fact, concomitant with this negative band, two positive bands are observed in the spectra at 2025-2019 and 1372 cm^{-1} corresponding to (adsorbed) CO and HCO_3^-, respectively. Both CO and bicarbonate (CO_2) can be suggested as products from methanol direct oxidation oxidation[31] and are observed at potentials higher than 0.2 V vs. SCE.

The CO related band around 2020 cm^{-1} is potential dependent as expected from adsorbed CO species and shifts 20 cm^{-1} V^{-1}. This band has been reported in the literature, for aqueous solutions and negative applied potentials (bellow the potential of zero charge) as CO adsorbed on metallic copper atoms[32,33].

The band at 2341 cm^{-1} is due to O-C-O stretching from CO_2. Unfortunately, as our specular compartment is not under vacuum, fluctuation of the CO_2 and water vapor content in the chamber can exist and affect the intensity of this band (positive or negative), making the interpretation of the potential formation of this possible product difficult. However, when CO_2 is dissolved in liquid a single band is observed instead of a double band. In Figure 2B the single band is therefore indicative of CO_2 in solution produced from methanol oxidation. The double band observed in Figure 2A is attributed to gas phase CO_2 in the specular compartment which may be obscuring a single positive band. Additionally, the presence of the bicarbonate band indicates that CO_2 is formed from methanol oxidation at the Cu electrode when the applied potential is higher than 0.2 V vs. SCE in both Figure 2A and B.

When the spectroelectrochemical cell is saturated with CO, the spectra (Figure 2B) change. The most prominent difference is the observation of a positive vibrational feature at 2106 cm^{-1} and a negative one at 1646 cm^{-1}. The latter is due to water oxidation in the thin layer, while the former band at 2106 cm^{-1} should be related with a CO species as it falls in the vibrational region where carbonyl bands are expected. In fact, such a band has been ascribed in literature to the formation of a Cu(I)CO complex in solution[29,34,35]. Furthermore, the band does not change with the applied potential, suggesting that it is indeed related with a solution species.

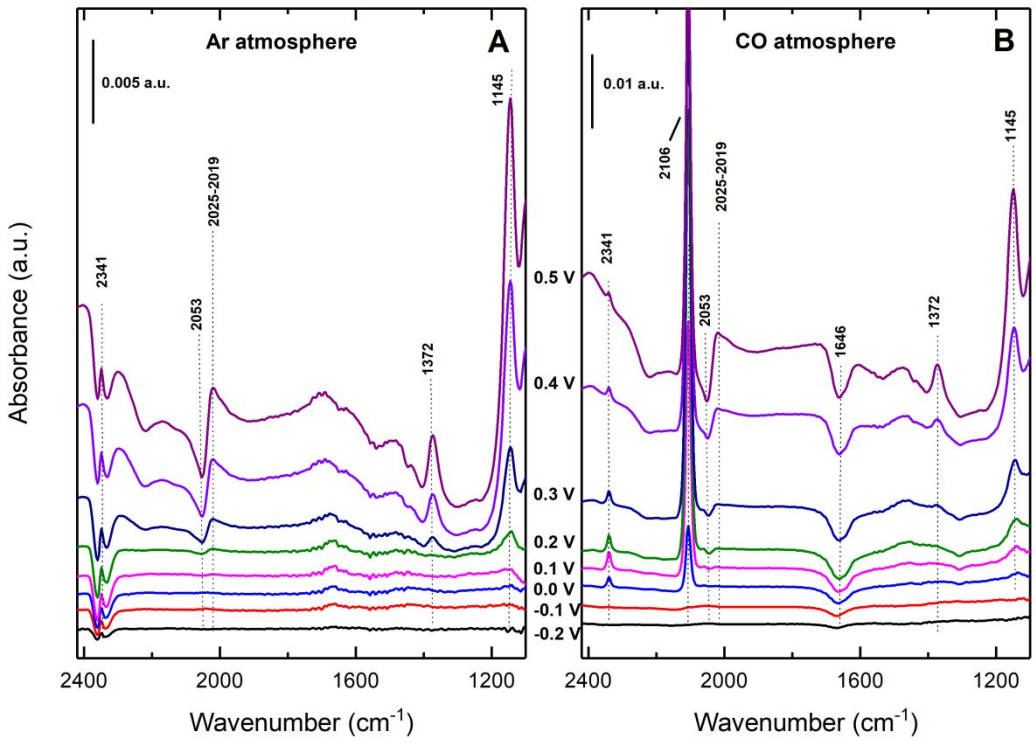

Figure 2. Infrared spectroelectrochemistry. Thin-film spectra for a copper electrode in (A) argon and (B) CO saturated electrolyte solutions of 0.1 M $NaClO_4$/methanol. Spectra were acquired from -0.2 in steps of 0.1 up to 0.5 V vs SCE, at 100 interferograms per spectrum and 8 cm^{-1} resolution. The backgrounds were recorded at -0.2 VSCE in the respective saturated solution.

In Figure 3, the integrated band area of the peak at 2106 cm^{-1} as a function of electrode potential is presented. Integration of the Cu(I)CO band area provides a qualitative measure of the quantity of the species present at a given potential. The Cu(I)CO band can be observed in the spectra at potentials as low as 0 V vs. SCE, increasing in intensity up to 0.2 V vs. SCE and then decreasing. Most likely, copper dissolution is initiated at 0 V vs. SCE forming Cu(I) in solution, that in the presence of CO produces a cuprous CuCO species. This electrochemical activity correlates with the CO-induced oxidation peak Ox3, in the CV of Figure 1

From 0.3 V vs. SCE onwards, both Cu(I) oxidation to Cu(II) and CO oxidation to CO_2 begin, decreasing the amount of Cu(I)CO species in solution, as observed from the lower intensity of the FTIR band at potentials higher than 0.3 V. When the electrode potential is higher than 0.2 V vs. SCE, bands similar to those observed in the absence of CO, are observed (band observed at 2341 cm^{-1} and bicarbonate band at 1372 cm^{-1}). These bands are probably due to methanol and CO oxidation to CO_2.

There is no evidence of DMC formation on the surface of the copper electrode, as neither vibrational features for DMC nor the methoxy surface intermedate are observed[24,36].

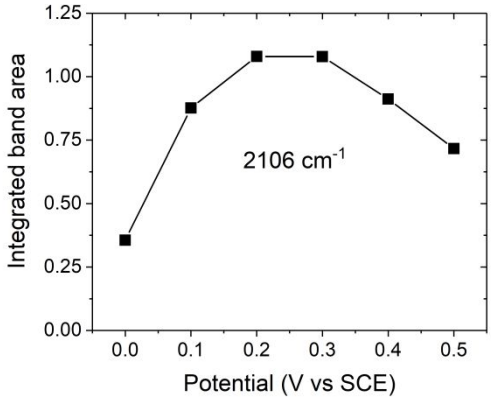

Figure 3. The $[CuCO]^+$ 2106 cm-1 integrated carbonyl band area at each applied potential from FTIR measurements provides a qualitative measure of the quantity of CuCO present at the different potentials. The potentials were applied from low to high potential.

Constant-potential electrolysis.

Constant-potential electrolysis was used to investigate potential dependent synthesis reactions. In these experiments, a selected potential was held for a set duration, after which, product analysis was performed. The electrolysis potential is held long enough to generate appreciable quantities of product for detection.

Based on the cyclic voltammograms of the copper electrode in Figure 1, a region of electrochemical activity is observed between 0 and 0.4 V_{SCE} for the CO/methanol system. In

addition to that, the recorded spectra in Figure 2 show that an interesting copper complex is being formed in this same potential range. In order to investigate the activity of the copper electrode and therewith, the CuCO species, for DMC synthesis, we performed electrolysis in this potential region. We focused our subsequent investigation on selectivity towards DMC production, Faradaic efficiency (FE) and potential dependence. The FE is determined by quantifying the charge generated for the DMC reaction and relating that to the total charge generated during the electrolysis.

Figure 4A shows the generated current densities, normalized to the geometric surface area (geo) of the electrode, for each electrolysis-potential. Good stability is obtained over the course of the experiment, after an initial induction period of approximately 5 minutes. The stabilized current densities were in the range of 0.1 to 4.5 mA cm^{-2}_{geo}. The trend in current densities follows that of the CV, where the peak in current density is between 0.2 and 0.4 V. It can also be seen that the CuCO band area (Figure 3) shows a similar trend as well, where the current density is highest, the reaction rate of formation is highest and so is the band intensity.

Analysis of the electrolyte solution immediately after the experiment revealed that DMC had not been produced, which is in agreement with the FTIR measurements (Figure 2). However, the samples were monitored over the course of 70 days and shortly after the experiment (1-2 days), DMC was present in the solution and its concentration slowly increased with time. In Figure 4B, the DMC concentration on day 3 and day 70 after the electrolysis is shown, where less than 5μM was detected on day 3 for each potential and by day 70, up to 24 μM DMC was detected. The DMC synthesis was initiated by the electrolysis and completed in solution until a maximum DMC concentration was reached. The insert in Figure 4B shows that the reaction starts to plateau at approximately day 40. The stability of the intermediate and slowness of the synthesis reaction, may be related to the stabilizing effect of the CO ligand, which is known to impart stability to copper perchlorate in solution[37].

There is synthesis activity for DMC in the same applied potential range as seen for the CO-induced CV oxidation peak and for CuCO formation, that is between 0 and 0.4 V_{SCE}. The highest concentrations were at 0.1 and 0.2 V. This potential-dependent and post-electrolysis formation of DMC indicates that an indirect electrochemical synthesis is taking place, through an electrochemically generated CuCO species. The reaction is selective for DMC as no other possible products were detected, as defined earlier.

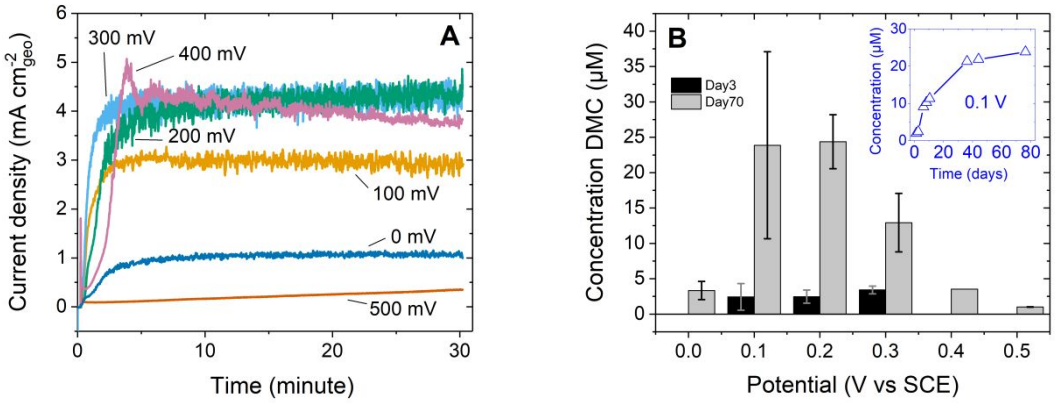

Figure 4. Electrochemical synthesis. (A) constant potential electrolysis geometric current densities for a copper disk electrode. Experiments were performed in CO saturated 0.1 M $NaClO_4$/methanol electrolyte solution each for 30 minutes, the counter electrode was copper mesh and the reference potential was the SCE. (B) concentration of DMC at 3 and 70 days after electrolysis. (B, insert) change of DMC concentration with time since the day of electrolysis, shown for 0.1 V vs. SCE. Duplicate or triplicate measurements at all potentials were performed, except 0.4 V vs. SCE and error bars show one standard deviation from the mean value.

Selectivity analysis.

The efficiency of charge passed, the Faraday efficiency (FE), for DMC formation is shown for day 3 and day 70 after electrolysis Figure 5A. The FE is in the range of 1-6% for the applied potentials tested. Therefore, even though there is a high selectivity for DMC, the majority of the CuCO species formed is utilized for another reaction or is deactivated.

The electrochemically-generated CuCO species is observed in the same potential region where DMC is formed, it is therefore hypothesized herein, that this Cu(I) species is the initiator for DMC synthesis from CO and methanol. The selectivity observed for DMC versus other possible products, indicates that the CuCO species is highly selective for DMC and Cu(I) is indeed well known for having a high selectivity for DMC synthesis in heterogeneous catalysis[15].

The production and FE of DMC is therefore directly related and limited to the FE of Cu(I), since the Cu(I) species is the precursor to DMC. Additionally, the yield of DMC will be related to, and limited by, the efficiency of the post-electrolysis homogeneous reaction. Therefore, the degree of Cu(I) dissolution into the electrolyte solution may elucidate the efficiency of the homogeneous reaction. Chemical analysis was performed on the electrolyte solutions to investigate the copper content. In Figure 5, the Cu concentration in the electrolysis solutions are presented. The concentration increases from 0.0 to 0.2 V vs. SCE and then stays relatively constant up until 0.4 V vs. SCE. Due to the low current generated at 0.5 V vs. SCE the quantity of copper in solution could not be determined as the signal was below the detection limit. Relating the observed Cu concentrations from 0 to 0.4 V vs. SCE to the charge passed during electrolysis shows close to 100% FE for the one electron oxidation reaction of Cu to Cu(I) Figure 5, suggesting a significant loss of the bulk electrode. However, a proportion of the current is likely to be due to the oxidation of Cu and Cu(I) to Cu(II), especially at more positive potentials. The chemical analysis performed only provides the concentration of copper and not the oxidation state. Therefore, the current density generated may be partly due to a combination of different Cu oxidation reactions as well as solvent oxidation reactions which were indicated by the spectroelectrochemistry results.

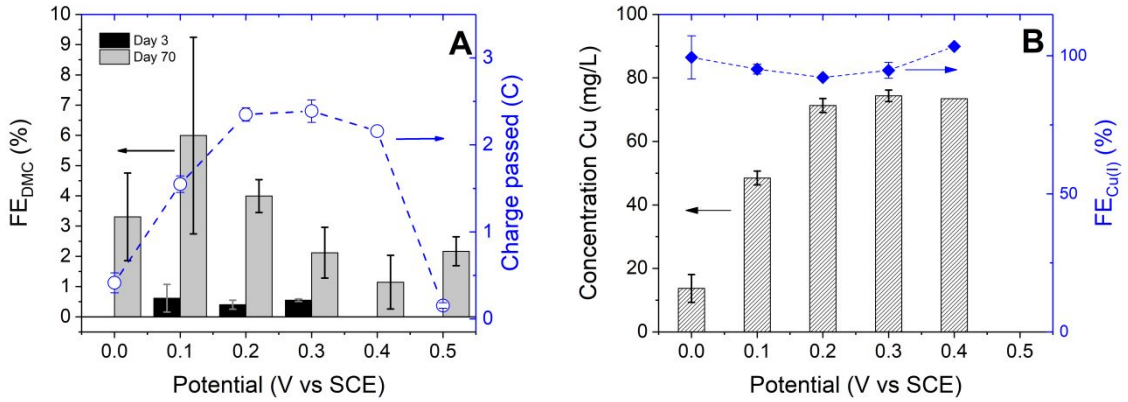

Figure 5. (A) Faraday efficiency (FE) for DMC and total charge passed during electrolysis at each applied potential of 30 minutes. FE is shown for both 3 and 70 days after electrolysis. (B) Concentration of copper in the electrolyte solution after electrolysis and resulting FE based on one electron oxidation of Cu to Cu(I). Copper determination at 0.5 V vs. SCE was below the detection limit and is therefore not shown. The resulting error in concentration of 1-2 replicate measurements at all potentials except 0.4 V vs. SCE are shown as one standard deviation from the mean value. At 0.4 the error of calibration is presented.

As the FE is close to 100% for Cu(I) formation between 0.1 and 0.4 V vs. SCE and features in the CV and spectroelectrochemical data show that the Cu(I) is formed from 0 up until 0.5 V, we identify the Cu(I)CO as the electrochemically generated, active and selective, species for DMC synthesis. Since the formation of Cu(I)CO appears to be highly efficient, it is likely that it is the homogenous step that is the limiting factor for DMC formation. It is observed that the CuCO reacts slowly, peaking around day 40 (Figure 4B insert) with a low FE. Oxidation of methanol to methoxy must occur in order to form DMC with the $CuCO^+$ intermediate. Therefore, based on Equation 2, where molecular oxygen is the oxidant, a tentative homogeneous reaction mechanism is presented by Equation 4, Equation 5 with the electrochemical step shown by Equation 6.

Equation 4

$$[CuCO]^+ + 2CH_3OH + ½O_2 \rightarrow [Cu(OCH_3)_2CO]^+ + H_2O$$

Equation 5

$$[Cu(OCH_3)_2CO]^+ \rightarrow Cu^+ + (CH_3O)_2CO$$

Where the $[CuCO]^+$ intermediate is generated electrochemically by:

Equation 6

$$Cu + CO \xrightarrow{E\ (0.0 - 0.4\ V_{SCE})} [CuCO]^+ + e^-$$

The homogeneous reactions occur in a sealed environment with CO and air. The CO originating from saturation of the electrolyte solution during electrolysis and the air (i.e. oxygen) from inevitable introduction during sample collection. The slow homogenous process may then be due to poor kinetics, low oxygen exposure or a combination of the two. Additional tests with increased oxygen exposure however, did not result in the immediate formation of DMC, therefore, slow kinetics may be the underlying problem for this reaction and further studies are required.

Due to the complexity of the electrochemical synthesis of DMC under these conditions, the technique is not a viable one for production before significant optimization is performed. However, these initial synthesis results also highlight the complexities and difficulties of investigating electrochemical reactions. In the instance that a homogenous step is quick for chemical formation, an indirect electrochemical synthesis may be mistaken for an electrocatalytic synthesis. This will impact analysis and optimization strategies and may be relevant for other investigations of electrocatalytic reactions, such as CO_2 reduction[38,39].

CONCLUSIONS

The combination of the experimental techniques of FTIR, constant potential electrolysis and HS-GS-MS has allowed us to study and understand the electrochemical synthesis of DMC on copper in detail. Our results show that copper does not act as a direct electrocatalyst for methanol carbonylation to DMC, rather, it acts as an indirect electrochemical catalyst. The spectroelectrochemical measurements do not show adsorbed methoxy, a known intermediate for direct electrochemical synthesis of DMC. The electrolysis tests, show that DMC is not immediately formed during synthesis. Interestingly, DMC was subsequently formed in the electrolyte solution. By using FTIR we observed a copper carbonyl (CuCO) formed by oxidative dissolution of the electrode in a CO saturated electrolyte solution. Dissolution to CuCO was found to be highly active and efficient with almost 100% FE and high and stable current densities for its generation. Formation of CuCO occurred over a wide potential range, from 0-0.5 V vs SCE. By using HS-GC-MS, we determined that DMC was formed in the electrolyte in the same potential range as the CuCO species was formed. The resulting current efficiency for DMC suffers from an inefficient chemical step and is on the order of 5% and is therefore not yet a viable method of DMC production. However, as yet, no optimization of the chemical step has been attempted. We concluded that the electrochemically generated CuCO species is active and selective for DMC synthesis in solution, by an indirect electrochemical mechanism.

DFT analysis initiated our experimental investigation of copper as an electrocatalyst and lead to the discovery of an indirect electrochemical synthesis route for DMC. The simulation is limited in the absence of known competing reactions, such as that of copper dissolution to from CuCO. We therefore emphasize the necessity of feed-back loops from theory and experiment to further develop the predictive technique, as one approach advances the other.

EXPERIMENTAL SECTION

Chemicals.

The electrolyte was $NaClO_4.H_2O$ (VWR, AnalaR NORMAPUR, ≥99.0%) dissolved in methanol (ultrapure, spectrophotometric grade 99.8 + % Alfa Aesar) to form a 0.1 M solution of $NaClO_4$/methanol. This electrolyte was used for all electrochemical measurements. Gasses used were argon (Air Liquide, Alphagaz 1.0, 99.999%) and carbon monoxide (Air Liquide, >99.95). All chemicals were used as received from the supplier.

Electrochemical measurements.

The cyclic voltammetry and electrolysis tests were performed in a three electrode divided H-cell connected to a potentiostat (Nordic EC ECi-200). The reference potential was a saturated calomel electrode (SCE) and the counter electrode was copper mesh. The working electrode for CV experiments consisted of a copper wire. The working electrode for electrolysis measurements consisted of a copper disk of 6.35 mm diameter x 3 mm height placed in a Teflon holder (Figure S3). The disk was flush with the end of the holder to produce a geometric surface area of 0.32 cm^2 which used to calculate the current density, J in mA cm^{-2}_{geo}. Before each experiment, the electrode was polished until a smooth mirror like surface was visible by 1μM then 0.3μM aluminum oxide suspension. The electrode was rinsed and solicited with ultrapure water between polishes. Finally, the electrode was sonicated in methanol and left to dry before electrochemical measurements were performed.

All compartments of the cell contained the same electrolyte solution with the working electrode compartment containing a measured 20 mL. The solution in the working electrode compartment was bubbled with either argon or carbon monoxide. To insure complete saturation of the electrolyte solution during electrolysis, CO at atmospheric pressure was continuously

bubbled. Each electrolysis test was performed for 30 minutes, after which, the electrolyte solution was collected for analysis in crimp sealed vials and were kept in these vials for HSGCMS analysis. During the experiment there is an over pressure of CO which results in the purging of air out of the cell, however, when the samples are collected, the lid of the H-cell must be opened and the bubbling of CO stopped, therefore, air is also contained within the vials. Between each electrolysis text, the cell was thoroughly rinsed with ultrapure water and methanol, and then dried. All experiments were performed at room temperature. A diagram of the cell used for electrochemical measurements can be found in the Supplementary Information.

Chemical analysis.

Quantitative chemical analysis was performed by an Agilent headspace sampler connected to a gas chromatograph with a mass spectrometry detector (HS-GC-MS). Chemical separation was achieved with an Agilent VF-624 column. The carrier gas was helium. The analysis method allowed for the observation of dimethyl carbonate, dimethyl oxalate, methyl formate, dimethoxy methane and dimethyl ether, tested by analyzing prepared reference solutions for mass spectra and retention time matches.

Determination of the copper concentration was performed using an inductively coupled plasma-mass spectrometer (ICP-MS). External calibration was performed with standards of known concentration. Samples were diluted in $2\%_{vol}$ HNO_3 prior to analysis. Further details on calibration and analysis can be found in the Supplementary Information.

The Faradaic efficiency (FE) is calculated by,

$$FE_i = \frac{eFn_i}{Q}$$

where e is the number of electrons transferred per mole of product, F is the Faraday constant in C mol^{-1}, n_i is the quantity of product i in mol and Q is the amount of charge passed during the electrolysis in C.

Spectroelectrochemistry.

For the spectroelectrochemistry measurements, a Thermo Fisher Nicolet 6700 spectrometer, equipped with a specular reflectance unit (VeeMAX II, PIKE Technologies) and a MCT detector was used. The experiments were performed in external reflection mode with a thin-layer configuration, using a glass three electrode spectroelectrochemical cell as described elsewhere[40]. The reference electrode potential as the SCE and counter electrode was platinum foil. The copper electrode was pressed against a CaF_2 prism at a controlled potential (-0.2 V vs. SCE) where a reference spectrum was obtained. Then, the electrode potential was stepped, successively to the sample potential where the sample spectra were recorded. The final spectra are presented as $(R-R_0)/R_0$, where R and R_0 is the reflectance at the sample and reference potential, respectively. Therefore, for the results presented in this work mean that positive bands in the spectra correspond to species with increased concentration and negative band to species with lower concentration in the sample potential, compared to the reference. Each spectrum corresponds to the collection of 100 scans with a resolution of 8 cm^{-1} which takes approximately 1 minute to complete. All measurements were recorded at room temperature.

ASSOCIATED CONTENT

Supporting Information. The following file is available free of charge.

Chemical quantification and electrolysis cell setup design (PDF).

AUTHOR INFORMATION

Corresponding Authors

*E-mail:

maria.escudero@chem.ku.dk

matthias.arenz@dcb.unibe.ch

jan.rossmeisl@chem.ku.dk

Present Addresses

†Avantium, Zekeringstraat 29, 1014 BV, Amsterdamn, Netherlands

Notes

The authors declare no competing financial interest.

ACKNOWLEDGEMENTS

We acknowledge financial support from Innovation Fund Denmark (Grand Solutions ProActivE 5124-00003 A).

ABBREVIATIONS

CV, cyclic voltammetry; HSGCMS, headspace sampler gas chromatograph mass spectrometer; FE, Faradaic efficiency.

REFERENCES

(1) Sequeira, C. A. C.; Santos, D. M. F. Electrochemical Routes for Industrial Synthesis. *J. Braz. Chem. Soc.* **2009**, *20*, 387–406.

(2) Frontana-Uribe, B. A.; Little, R. D.; Ibanez, J. G.; Palma, A.; Vasquez-Medrano, R. Organic Electrosynthesis: A Promising Green Methodology in Organic Chemistry. *Green Chem.* **2010**, *12*, 2099.

(3) Cardoso, D. S. P.; Šljukić, B.; Santos, D. M. F.; Sequeira, C. A. C. Organic Electrosynthesis: From Laboratorial Practice to Industrial Applications. *Org. Process Res. Dev.* **2017**, 1213–1226.

(4) Aricò, F.; Tundo, P. Dimethyl Carbonate as a Modern Green Reagent and Solvent. *Russ. Chem. Rev.* **2010**, *79*, 479–489.

(5) Tundo, P.; Selva, M. The Chemistry of Dimethyl Carbonate. *Acc. Chem. Res.* **2002**, *35*, 706–716.

(6) Ono, Y. Dimethyl Carbonate for Environmentally Benign Reactions. *Pure Appl. Chem.* **1996**, *68*, 367–375.

(7) Ono, Y. Catalysis in the Production and Reactions of Dimethyl Carbonate, an Environmentally Benign Building Block. *Appl. Catal. A Gen.* **1997**, *155*, 133–166.

(8) Centi, G.; Perathoner, S. From Green to Sustainable Industrial Chemistry. In *Sustainable Industrial Chemistry*; Cavani, F., Centi, G., Perathoner, S., Trifiró, F., Eds.; WILEY-VCH: Weinheim, 2009; p 599.

(9) Selva, M.; Perosa, A. Green Chemistry Metrics: A Comparative Evaluation of Dimethyl Carbonate, Methyl Iodide, Dimethyl Sulfate and Methanol as Methylating Agents. *Green Chem.* **2008**, *10*, 457.

(10) Li, Q.; Chen, J.; Fan, L.; Kong, X.; Lu, Y. Progress in Electrolytes for Rechargeable Li-Based Batteries and Beyond. *Green Energy Environ.* **2016**, *1*, 18–42.

(11) Nitta, N.; Wu, F.; Lee, J. T.; Yushin, G. Li-Ion Battery Materials: Present and Future. *Mater. Today* **2015**, *18*, 252–264.

(12) UBE Industries. Ube Industries Licenses DMC Technology and Agrees to Establish

Joint Venture for High-Purity DMC http://www.ube-ind.co.jp/ube/en/news/2015/20160316_01.html (accessed Mar 12, 2018).

(13) Di, M. N.; Fusi, C.; Rivetti, F.; Sasselli, G. Process for Producing Dimethyl Carbonate. European Patent EP0460732A1, 1991.

(14) Miyazaki, H.; Shiomi, Y.; Fujitus, S.; Masunaga, K.; Yanagisawa, H. Process for the Preparation of Oxalic Acid Diesters. United States Patent 4384133, 1982.

(15) Santos, B. a. V.; Silva, V. M. T. M.; Loureiro, J. M.; Rodrigues, A. E. Review for the Direct Synthesis of Dimethyl Carbonate. *ChemBioEng Rev.* **2014**, *1*, 214–229.

(16) Otsuka, K.; Yagi, T.; Yamanaka, I. Synthesis of Dimethyl Carbonate by Electrolytic Carbonylation of Methanol in the Gas Phase. *Chem. Soc. Japan* **1994**, No. 3, 495–498.

(17) Otsuka, K.; Yagi, T.; Yamanaka, I. Dimethyl Carbonate Synthesis by Electrolytic Carbonylation of Methanol in the Gas Phase. *Electrochim. Acta* **1994**, *39*, 2109–2115.

(18) Pacheco, M. A.; Marshall, C. L. Review of Dimethyl Carbonate (DMC) Manufacture and Its Characteristics as a Fuel Additive. *Energy & Fuels* **1997**, *11*, 2–29.

(19) Funakawa, A.; Yamanaka, I.; Otsuka, K. Active Control of Methanol Carbonylation Selectivity over Au/Carbon Anode by Electrochemical Potential. *J. Phys. Chem. B* **2005**, *109*, 9140–9147.

(20) Funakawa, A.; Yamanaka, I.; Otsuka, K. High Efficient Electrochemical Carbonylation of Methanol to Dimethyl Carbonate by Br2⁄Br− Mediator System over Pd⁄C Anode. *J. Electrochem. Soc.* **2006**, *153*, D68.

(21) Yamanaka, I.; Funakawa, A.; Otsuka, K. Selective Carbonylation of Methanol to Dimethyl Carbonate by Gas–Liquid–Solid-Phase Boundary Electrolysis. *Chem. Lett.*

2002, *2*, 448–448.

(22) Yamanaka, I.; Funakawa, A.; Otsuka, K. Electrocatalytic Synthesis of DMC over the Pd/VGCF Membrane Anode by Gas-Liquid-Solid Phase-Boundary Electrolysis. *J. Catal.* **2004**, *221*, 110–118.

(23) Funakawa, A.; Yamanaka, I.; Takenaka, S.; Otsuka, K. Selectivity Control of Carbonylation of Methanol to Dimethyl Oxalate and Dimethyl Carbonate over Gold Anode by Electrochemical Potential. *J. Am. Chem. Soc.* **2004**, *126*, 5346–5347.

(24) Figueiredo, M. C.; Trieu, V.; Eiden, S.; Koper, M. T. M. M. Spectro-Electrochemical Examination of the Formation of Dimethyl Carbonate from CO and Methanol at Different Electrode Materials. *J. Am. Chem. Soc.* **2017**, *139*, 14693–14698.

(25) Otsuka, K. Electrolytic Carbonylation of Methanol over the CuCl2 Anode in the Gas Phase. *J. Electrochem. Soc.* **1995**, *142*, 130.

(26) Cipris, D.; Mador, I. L. Anodic Synthesis of Organic Carbonates. *J. Electrochem. Soc.* **1978**, *125*, 1954–1959.

(27) Heli, H.; Jafarian, M.; Mahjani, M. G.; Gobal, F. Electro-Oxidation of Methanol on Copper in Alkaline Solution. *Electrochim. Acta* **2004**, *49*, 4999–5006.

(28) Abd El Haleem, S. M.; Ateya, B. G. Cyclic Voltammetry of Copper in Sodium Hydroxide Solutions. *J. Electroanal. Chem* **1981**, *117*, 309–319.

(29) Brooksby, P. A.; McQuillan, A. J. Oxidative IR Spectroelectrochemistry of Copper in Methanol Containing Carbon Monoxide. *Langmuir* **2014**, *30*, 14337–14342.

(30) Marshall, A. T.; Golovko, V.; Padayachee, D. Influence of Gold Nanoparticle Loading in Au/C on the Activity towards Electrocatalytic Glycerol Oxidation. *Electrochim. Acta*

2015, *153*, 370–378.

(31) Housmans, T. H. M.; Wonders, A. H.; Koper, M. T. M. Structure Sensitivity of Methanol Electrooxidation Pathways on Platinum: An on-Line Electrochemical Mass Spectrometry Study. *J. Phys. Chem. B* **2006**, *110*, 10021–10031.

(32) Hori, Y.; Koga, O.; Yamazaki, H.; Matsuo, T. Infrared Spectroscopy of Adsorbed CO and Intermediate Species in Electrochemical Reduction of CO2 to Hydrocarbons on a Cu Electrode. *Electrochim. Acta* **1995**, *40*, 2617–2622.

(33) Shaw, S. K.; Berná, A.; Feliu, J. M.; Nichols, R. J.; Jacob, T.; Schiffrin, D. J. Role of Axially Coordinated Surface Sites for Electrochemically Controlled Carbon Monoxide Adsorption on Single Crystal Copper Electrodes. *Phys. Chem. Chem. Phys.* **2011**, *13*, 5242.

(34) Salimon, J.; Hernández-Romero, R. M.; Kalaji, M. The Dynamics of the Conversion of Linear to Bridge Bonded CO on Cu. *J. Electroanal. Chem.* **2002**, *538–539*, 99–108.

(35) Hernández-R, R. M.; Kalaji, M. Electrochemical Reactions of CO on Polycrystalline Copper Electrodes. *J. Electroanal. Chem.* **1997**, *434*, 209–215.

(36) Rodriguez, P.; Kwon, Y.; Koper, M. T. M. The Promoting Effect of Adsorbed Carbon Monoxide on the Oxidation of Alcohols on a Gold Catalyst. *Nat. Chem.* **2012**, *4*, 177–182.

(37) Ogura, T. Complex Formation of Copper(I) Perchlorate with Ethylene or Carbon Monoxide in Water and Isolation of Related Complexes. *Inorg. Chem.* **1976**, *15*, 2301–2303.

(38) Kuhl, K. P.; Cave, E. R.; Abram, D. N.; Jaramillo, T. F. New Insights into the

Electrochemical Reduction of Carbon Dioxide on Metallic Copper Surfaces. *Energy Environ. Sci.* **2012**, *5*, 7050.

(39) Arán-Ais, R. M.; Gao, D.; Roldan Cuenya, B. Structure- and Electrolyte-Sensitivity in CO2 Electroreduction. *Acc. Chem. Res.* **2018,** https://pubs.acs.org/doi/10.1021/acs.accounts.8b00360.

(40) Iwasita, T.; Nart, F. C. In Situ Infrared Spectroscopy At Electrochemical Interfaces. *Prog. Surf. Sci.* **1997**, *55*, 271–340.

Table of Contents Graphic